INFORMATION EXTRACTION FROM IMPEDANCE SPECTRA: THEORETICAL PREDICTIONS AND IN VIVO VALIDATION FOR THE ORAL MUCOSA

I. Lacković and Z. Stare

Faculty of Electrical Engineering and Computing, University of Zagreb, Zagreb, Croatia

igor.lackovic@fer.hr

Abstract: The aim of our study was to investigate the relationship between widely used set of impedance indices (*MIX*, *PIX*, *RIX*, *IMIX*) and macroscopic tissue properties – tissue electrical conductivity σ and permittivity ε. The issues we addressed theoretically and experimentally are: i) are these indices mutually independent, ii) can they distinguish different tissue structure, iii) what is their coefficient of variation, and iv) are they sensitive to probe geometry being used for impedance measurement. For a tissue modeled as an isotropic dispersive monodomain we have shown theoretically that impedance phase does not depend on geometry of the impedance probe being used nor does the phase depend on the size of tissue sample. Therefore, normalization of phase in the form of *PIX* index is not necessary. We also demonstrated that *MIX*, *PIX*, *RIX*, *IMIX* do not depend on probe geometry. This was also proved with finite-element models. Preliminary experimental validation was performed for the oral mucosa where impedance magnitude and phase were measured with two intraoral probes of different geometries. The results, as expected, showed considerable difference in impedance magnitude and negligible difference in impedance phase for the same anatomical location.

Introduction

Impedance spectroscopy is a noninvasive technique used for tissue characterization. Since impedance measurements are performed over a frequency range that spans several decades, there is a need for data reduction and information extraction from the vast amount of impedance data.

The simplest way of data reduction is some sort of impedance indexing [1]. A set of four impedance indices *MIX*, *PIX*, *RIX* and *IMIX* has been used in a great number of studies aimed at performing 'electronic biopsy' of skin lesion and characterization of pathophysiological status of the oral mucosa [1-5]. Our earlier studies pointed to some weaknesses of these indices [6, 7]. Undoubtedly, optimal impedance indices that are sensitive enough to distinguish different tissue structure, and that have at the same time not a too large variation are not easy to find.

More sophisticated methods of information extraction from impedance spectra include fitting the impedance data to some model (e.g. Cole-Cole, lumped RC model, etc.), use of neural networks, principal component analysis and so on [8-10]. Features extracted in this way seem to better represent the underlying information in the impedance spectra, but not necessarily.

The aim of our study was to establish the relationship between widely used impedance indices *MIX*, *PIX*, *RIX*, *IMIX* and macroscopic tissue properties – tissue electrical conductivity σ and permittivity ε. The issues we are addressing theoretically and experimentally are: i) are these indices mutually independent, ii) can they distinguish different tissue structure, iii) what is their coefficient of variation, and iv) are they sensitive to probe geometry being used for impedance measurement?

Materials and Methods

For theoretical considerations we used indices as defined in [1]:

$$MIX = \frac{|Z|_{20\,\mathrm{kHz}}}{|Z|_{500\,\mathrm{kHz}}} \tag{1}$$

$$PIX = \varphi_{20\,\mathrm{kHz}} - \varphi_{500\,\mathrm{kHz}} \tag{2}$$

$$RIX = \frac{\mathrm{Re}\,Z_{20\,\mathrm{kHz}}}{|Z|_{500\,\mathrm{kHz}}} \tag{3}$$

$$IMIX = \frac{\mathrm{Im}\,Z_{20\,\mathrm{kHz}}}{|Z|_{500\,\mathrm{kHz}}} \tag{4}$$

For numerical evaluation we constructed finite-element models and used them to calculate impedance magnitude and phase for three different probe geometries: our coaxial bipolar intraoral used in previous study [6], modification of this probe having smaller radii and a probe comprised of two parallel plates, Figure 1. Coaxial probes had the following electrode radii: CP-1: $\{r_1, r_2, r_3, r_4\}$= {0.8, 1.0, 3.65, 4} mm, CP-2: $\{r_1, r_2, r_3, r_4\}$= {0.2, 0.8, 2.3, 2.5} mm. Parallel plates had radius 4 mm.

We modeled the tissue as an isotropic dispersive monodomain i.e. both electrical conductivity σ and permittivity ε were allowed to be frequency dependent. In this way we account for different microscopic tissue structure and different relaxation processes occurring in tissues (α-, β-, and γ-dispersion). Thickness of tissue sample was 1 cm, while the diameter was 4 cm.

If current passes through a tissue, then throughout the tissue there will be a distribution of potential that is

ISSN: 1727-1983

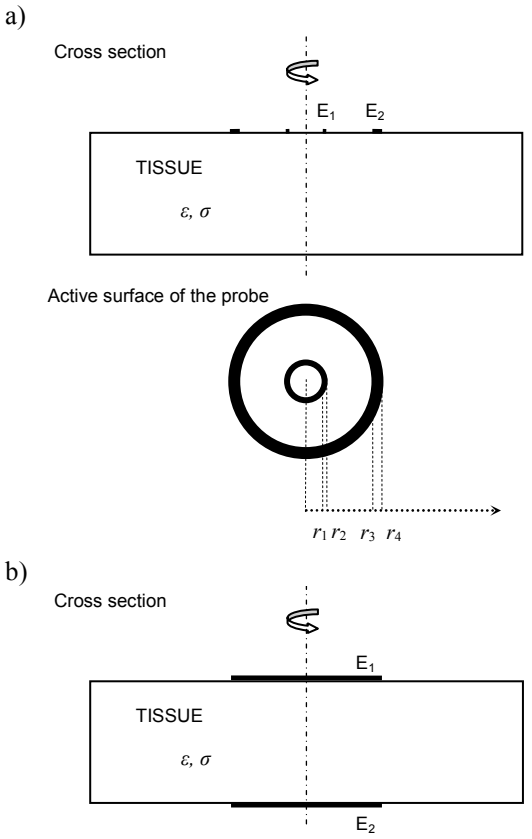

Figure 1: Probe geometry. a) coaxial probe (r_1 and r_2 are the inner and outer radii of the electrode E_1; r_3 and r_4 are the same for the electrode E_2); b) parallel plates.

dependent on the distribution of conductivity and permittivity. Assuming quasistatic conditions and linear isotropic volume conductor, the electric potential u associated with AC current conduction satisfies:

$$-\nabla \cdot [(\sigma + j\omega\varepsilon)]\nabla u = 0 \tag{5}$$

where ω is the angular frequency. The first term is the contribution from conduction current density and the second is from displacement current density. In this formulation, the effect of current flow on electric field through induced magnetic field has been neglected. After this equation is solved, impedance is calculated by dividing complex potential difference between electrodes with small measuring current injected through the electrodes.

We used finite-element modeling environment FEMLAB 3.1 (Comsol AB, Sweden) interfaced with MATLAB 6.5 (The MathWorks, Inc., USA). Due to axial symmetry instead of full 3D modeling we chose 2D axisymmetic approach. Geometry was tessellated into nonuniform dense mesh of second order triangular elements (≈ 16000). Frequency was varied from 10 Hz to 10 MHz. Tissue permittivity and conductivity at different frequencies were taken from the literature [11].

Experimental procedure for intraoral impedance measurements was described previously [6]. Briefly, impedance was measured at various regions of the oral mucosa (tongue, hard palate, buccal mucosa, madibular gingiva) in the frequency range from 30 Hz to 1 MHz using HP 4284A precision LCR meter (Hewlett-Packard, USA). Data acquisition was controlled via HPIB from a laptop computer.

Results and discussion

By using the complex conductivity σ^* the impedance of a lossy dielectric can be expressed as:

$$Z = \frac{1}{\sigma^*}\frac{d}{A} = \frac{1}{\sigma + j\omega\varepsilon}\frac{d}{A} = \frac{\sigma - j\omega\varepsilon}{\sigma^2 + (\omega\varepsilon)^2}\frac{d}{A} \tag{6}$$

where d is the distance between two flat parallel faces of area A. Impedance magnitude |Z| is:

$$|Z| = \frac{1}{\sqrt{\sigma^2 + (\omega\varepsilon)^2}}\frac{d}{A} \tag{7}$$

and phase is:

$$\varphi = -\arctan\frac{\omega\varepsilon}{\sigma} \tag{8}$$

Note that the phase is dependent only on the frequency of the field ω and the physical properties of tissue (σ, ε) and is not dependent on the geometry factor (A/d). This has important implications. Theoretically, if tissue is treated as macroscopically homogenous and isotropic, then impedance phase measured with different electrodes should be equal. At cellular and subcellular level physical tissue properties are of course inhomogenous (e.g. conductivity of cell membranes is several orders of magnitude lower than intracellular or extracellular conductivity). However, this non homogenous microscopic structure maps into frequency dependence of macroscopic (bulk) tissue properties (i.e. dielectric dispersions) allowing us to use monodomain model of tissue.

By introducing eqn. (6) into eqns. (1)-(4) we derived following formulas relating impedance indices and tissue conductivity and permittivity:

$$MIX = \sqrt{\frac{\sigma^2 + (\omega\varepsilon)^2\big|_{500\text{ kHz}}}{\sigma^2 + (\omega\varepsilon)^2\big|_{20\text{ kHz}}}} \tag{9}$$

$$PIX = \arctan\frac{\omega\varepsilon}{\sigma}\bigg|_{500\text{ kHz}} - \arctan\frac{\omega\varepsilon}{\sigma}\bigg|_{20\text{ kHz}} \tag{10}$$

$$RIX = \sigma_{20\text{ kHz}}\frac{\sqrt{\sigma^2 + (\omega\varepsilon)^2\big|_{500\text{ kHz}}}}{\sigma^2 + (\omega\varepsilon)^2\big|_{20\text{ kHz}}} \tag{11}$$

$$IMIX = -(\omega\varepsilon)|_{20\text{ kHz}}\frac{\sqrt{\sigma^2 + (\omega\varepsilon)^2\big|_{500\text{ kHz}}}}{\sigma^2 + (\omega\varepsilon)^2\big|_{20\text{ kHz}}} \tag{12}$$

Here all parameters (i.e. σ, ε, and $\omega = 2\pi f$) preceding the vertical bar $|_{f\text{ kHz}}$ are taken at a given frequency f. We see that all indices depend only on tissue properties and frequency and are not dependent on the probe geometry. This property is very beneficial for practical

ISSN: 1727-1983

purpose. Namely, indices enable data normalization, allowing for the comparison of results obtained in similar studies performed with different impedance probes. Only normalization of phase in the form of *PIX* index seems unnecessary since phase by itself is inherently not dependent on geometry factor (see eqn. (8)).

It is also interesting to note that impedance indices are not mutually independent. Namely, as we have shown previously [7]:

$$RIX^2 + IMIX^2 = MIX^2 \qquad (13)$$

meaning that set of 4 indices is redundant.

Figure 2 compares calculated |Z| and φ from FEM simulations for three different probe geometries. Conductivity and permittivity were taken from impedance spectra for liver [11].

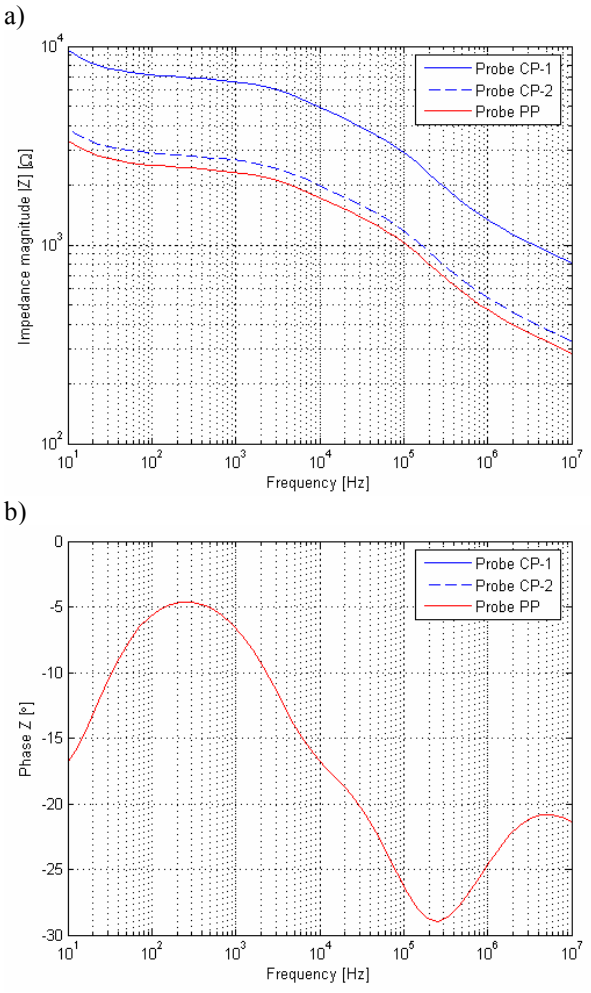

Figure 2: Impedance vs. frequency calculated for three different probe geometries: coaxial probes (CP-1 and CP-2) and parallel plates (PP). a) magnitude |*Z*|; b) phase Z (all three curves overlap)

The obtained numerical results confirm previous theoretical predictions that impedance phase is not dependent on probe geometry. Impedance magnitude, as expected, differs considerably for three different probes. However, the shape of magnitude spectra is the same for both the parallel plates and coaxial probes. Impedance indices calculated from impedance spectra shown in Figure 2 are equal for all three probes (CP-1, CP-2 and PP). Their values are: *MIX*=2.51, *PIX*=9.1, *RIX*=2.37, *IMIX*=-0.81. These numerical results are in full agreement with theory (eqns. (9)-(12)), and validate the hypothesis that all impedance indices (*MIX*, *PIX*, *RIX* and *IMIX*) do not depend on the geometry of the probe for impedance measurement. The above results hold under assumption of tissue being an isotropic monodomain.

Figure 3 presents calculated |*Z*| and φ for different tissues. These results were obtained by FEM simulations for coaxial probe CP-1.

Table 1 summarizes impedance indices calculated from impedance spectra of different tissues shown in Figure 3.

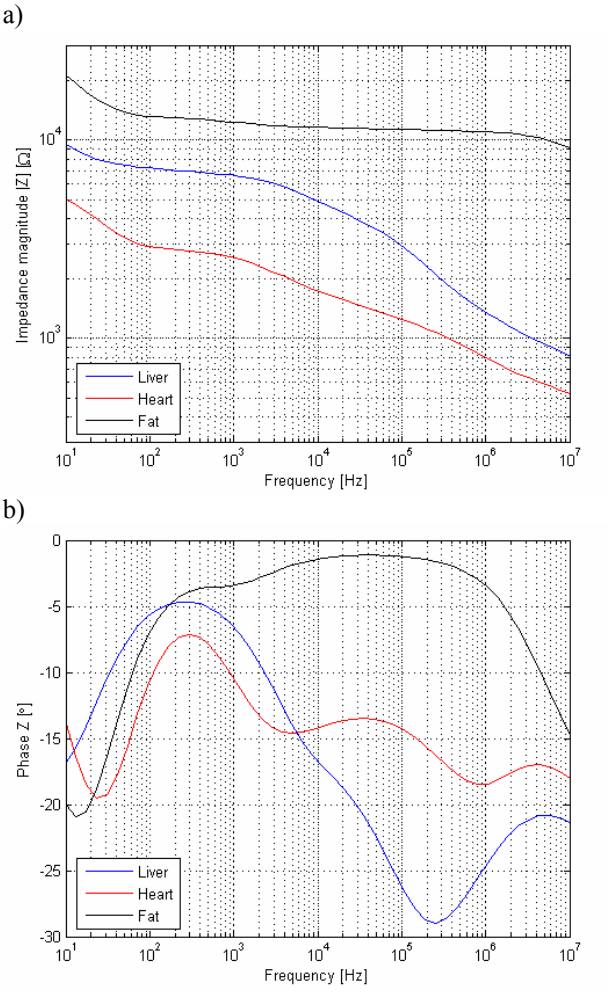

Figure 3: Impedance vs. frequency calculated for different tissues. a) magnitude |*Z*|; b) phase *Z*.

Table 1: Impedance indices for different tissues calculated from literature data

	MIX	*PIX*	*RIX*	*IMIX*
Liver	2.51	9.1	2.37	-0.81
Heart	1.63	4.1	1.58	-0.38
Fat	1.03	0.9	1.03	-0.02

ISSN: 1727-1983

Comparison of impedance indices given in Table 1 and impedance spectra shown in Figure 3 helps to evaluate the potential of impedance indices to differentiate between different tissue types. It is evident that impedance spectra (both $|Z|$ and φ) of liver, heart and fat markedly differ. Mapping from impedance spectra to impedance indices tend to reduce the differences. Potentially this could lead to lost of information. Index *PIX* seems to be the most critical in this respect.

Figure 4 shows measured impedance spectra at dorsal side of the tongue in one healthy subject. Impedance measurements were performed with coaxial probe CP-1 and with smaller probe CP-2. Measurements were repeated several times and data were averaged. This figure is to illustrate the influence of probe geometry on measured impedance in real *in vivo* experiment.

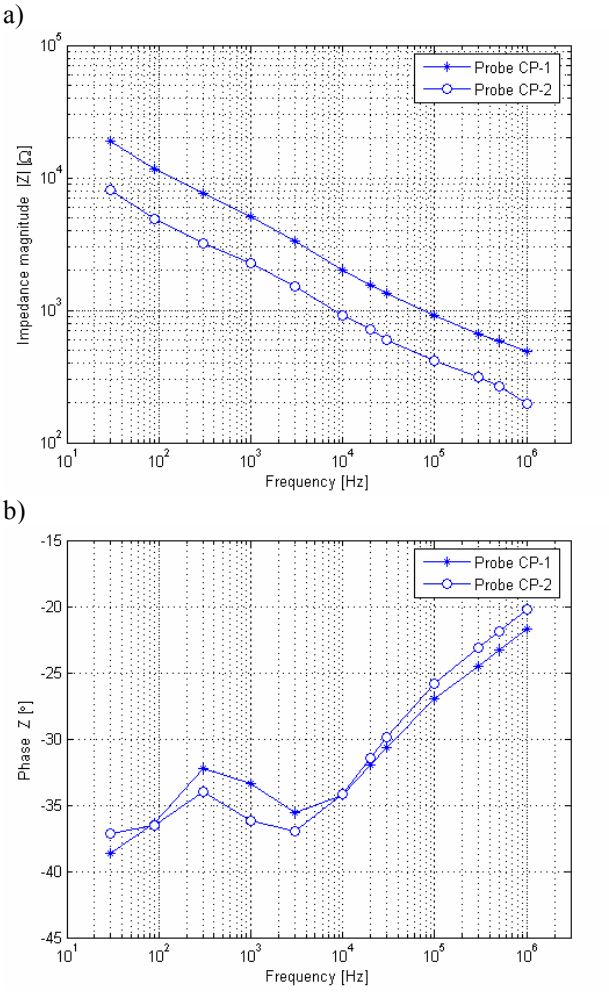

Figure 4: Impedance vs. frequency measured at dorsal side of the tongue with coaxial probes CP-1 and CP-2. a) magnitude $|Z|$; b) phase Z.

Experimental results seem to agree with theoretical predictions and result of simulations. We see that the impedance phase is much less sensitive to the probe size, than the impedance magnitude which differs considerably (more than 2 times). Discrepancies that exist are due to experimental constraints inherent to *in vivo* impedance measurements, electrode polarization, complex tissue structure and other factors that are not so easy to control. Thus, carefully performed measurements are needed to achieve acceptable repeatability. The impedance indices extracted from impedance spectra measured with two different coaxial electrodes agree well. However, variability of impedance data is considerable. Full validation would require measurement on a group of subjects at various regions of the oral mucosa with two different probes and in-depth statistical analysis.

Statistical analysis of impedance spectra and related impedance indices for the oral mucosa that we obtained experimentally in a previous study on a group of 20 subjects can be found in our previous publications [6, 7]. Present study enables to evaluate these results and the results of other research groups with deeper understanding.

Regarding the implications of our theoretical and simulation results to *in vivo* measurements we are aware that isotropic monodomain as a model may be questioned due to the layered structure of the oral mucosa. However, this has to be investigated using modeling at cellular level.

Moreover, the assumption that geometry factor is independent of frequency (i.e. that it is equal at 20 kHz and 500 kHz) was essential in our derivations of eqns. (9)-(12). This assumption is natural, although it can be violated in certain experimental conditions. This was seen experimentally as dependence of cell factor not only on geometry but also on the frequency [12].

Conclusions

Under the assumption that geometric factor (area/distance) does not change with frequency, and frequency is high enough that electrode polarization can be neglected, we derived expressions for *MIX*, *PIX*, *RIX* and *IMIX* as functions of tissue conductivity σ and permittivity ε.

For a tissue treated as an isotropic monodomain we have shown theoretically that impedance phase does not depend on geometry of the impedance probe being used nor does the phase depend on the size of tissue sample. Therefore, normalization of phase in the form of *PIX* index is not necessary. This was also proved with finite-element models. Finally, preliminary experimental validation for the oral mucosa was performed where impedance magnitude and phase were measured with two intraoral probes of different geometries. The results, as expected, showed considerable difference in impedance magnitudes and small difference in impedance phase for the same anatomical locations.

Practical implications of our results might be that for data reduction and information extraction from impedance spectra of the oral mucosa, a better choice would be to use *MIX* and phase angle at 100 kHz instead of four previously used indices *MIX*, *PIX*, *RIX* and *IMIX*.

ISSN: 1727-1983

Acknowledgement

The authors acknowledge Ivica Richter's help for all examinations and measurements in the oral cavity. Partial financial support for this research was provided by the Ministry of Education, Science and Sport of the Republic of Croatia (grant no. 0036007).

References

[1] OLLMAR, S. (1998): 'Methods of information extraction from impedance spectra of biological tissue, in particular skin and oral mucosa – a critical review and suggestions for the future', *Bioelectrochem. Bioenerget.*, **45**, pp. 157-160.

[2] OLLMAR, S., EEK, A., SUNDSTRÖM, F. AND EMTESTAM, L. (1995): 'Electrical impedance for estimation of irritation in oral mucosa and skin', *Med. Prog. Technol.*, **21**, pp. 29-37.

[3] NICANDER, I., RUNDQUIST L., AND OLLMAR, S. (1997): 'Electric impedance measurements at six different anatomic locations of macroscopically normal human oral mucosa', *Acta Odontol. Scan.*, **55**, pp. 88-93.

[4] NICANDER., I., AND OLLMAR, S. (1999): 'Electrical impedance related to structural differences in the skin and in the oral mucosa', *Med. Biol. Eng. Comput.*, **37** (suppl. 1), pp. 161-162.

[5] BEETNER, D.G., KAPOOR, S., MANJUNATH, S., ZHOU, X., AND STOECKER, W.V. (2003): 'Differentiation among basal cell carcinoma, benign lesions, and normal skin using electrical impedance', *IEEE Trans. Biomed. Eng.*, **50**, pp. 1020-1025.

[6] LACKOVIĆ, I., STARE, Z., RICHTER, I. (2002): 'Characteristics of the electrical impedance at various regions of normal oral mucosa', *IFMBE Proc.,* **3**, (Proc. EMBEC'02), pp. 138-139.

[7] LACKOVIĆ, I., STARE, Z., PROTULIPAC, T. (2003): 'On the applicability of electrical impedance indices to characterize the condition of the oral mucosa', Advances in Computational Bioengineering: Simulations in Biomedicine V, WIT Press, 2003, pp. 421-430.

[8] OLLMAR, S., NICANDER, I.,OLLMAR, J., AND EMTESTAM, L. (1997): 'Information in full and reduced data sets of electrical impedance spectra from various skin conditions, compared using a holographic neural network', *Med. Biol. Eng. Comput.*, **35**, pp. 415-419.

[9] DUA, R., BEETNER, D.G., STOECKER, W.V., AND WUNSCH, D.C. (2004): 'Detection of basal cell carcinoma using electrical impedance and neural networks', *IEEE Trans. Biomed. Eng.*, **51**, pp. 66-71.

[10] ABERG, P., NIKANDER, I., HANSON, J., GELADI P., HOLMGREN, U. AND OLLMAR., S. (2004): 'Skin cancer identification using multifrequency electrical impedance – a potential screening tool', *IEEE Trans. Biomed. Eng.*, **51**, pp. 2097-2102.

[11] GABRIEL, C., GABRIEL, S., AND CORTHOUT E. (1996): 'The dielectric properties of biological tissues: I. Literature survey', *Phys. Med. Biol.*, **41**, pp. 2231-2249.

[12] RIGAUD, B., MORUCCI, J.-P. AND CHAUVEAU, N. (1996): 'Impedance spectrometry', *Crit. Rev. Biomed. Eng.*, **24**, pp. 257-351.

ISSN: 1727-1983